

A numerical solution for a finite internally cracked plate using hybrid crack element method

Y.Z. Chen*

Division of Engineering Mechanics, Jiangsu University, Zhenjiang, Jiangsu, 212013
People's Republic of China

(Received May 25, 2011, Revised August 21, 2011, Accepted November 2, 2011)

Abstract. This paper provides a numerical solution for a finite internally cracked plate using hybrid crack element method (HCE). In the formulation, an inclined crack is placed in any place of a rectangular element and the complex variable method is used. The complex potentials are expressed in a series form, and several undetermined coefficients are involved. The complex potentials for the cracked rectangle are first suggested in this paper. Based on a variational principle, the element stiffness matrix can be evaluated. The next steps are same as in the usual finite element method. Several numerical examples with computed stress intensity factor and T-stress are presented.

Keywords: hybrid crack element; variational principle; complex variable method; stress intensity factor; T-stress

1. Introduction

Generally, the potential energy principle is used to formulate the element stiffness matrix in the finite element method (FE). It is evident that the admissible displacement field in each element should be such that it is not only continuous within the element but also compatible at the interelement boundaries. In earlier years, the concept of separately assuming displacements and stresses over different parts of the continuum was suggested (Pian 1964). The hybrid stress element (HSE) method was thus formulated. The relaxation of requirements of interelement displacement continuity and traction reciprocity in hybrid element method may provide some flexibility in the process of solution. Many possibilities of formulating the hybrid finite element were proposed (Day and Yang 1982, Pian and Chen 1982, Pian *et al.* 1983). A linear plane element was suggested, which is based on the hybrid Trefftz method (Choi *et al.* 2006). Four- and eight-node quadrilateral finite element models are devised for plane Helmholtz problems (Sze *et al.* 2010). Mixed 4-node elements based on the Hu-Washizu functional are developed for stress and strain representations in various coordinates (Wisniewski and Turska 2009).

Similar methods have been proposed more recently (Long *et al.* 2009). A 4-node hybrid stress-function membrane element with drilling degrees of freedom was developed based on the principle of minimum complementary energy (Cen *et al.* 2011). It was proved that the suggested hybrid

*Corresponding author, Professor, E-mail: chens@ujs.edu.cn

stress-function membrane element exhibited much improved numerical accuracy and robust performance. In particular, the element performs well even when the element shape degenerates into a triangle or concave quadrangle.

A collection in the field of the hybrid finite element method was published (Atluri *et al.* 1983). A hybrid-Trefftz element containing an elliptic hole was suggested (Dhanasekar *et al.* 2006). In the formulation, the trial functions for the assumed displacement-stress field are derived from an elasticity solution, which satisfy the traction free condition along the elliptic hole automatically.

The hybrid crack element (HCE) method was suggested by some pioneer researchers (Tong *et al.* 1973, Tong and Rossettos 1977). Summary and theoretical background for the hybrid and mixed finite element methods can be found from (Atluri *et al.* 1983). After using conformal mapping, complex potentials were derived to model the displacement-stress field for an edge cracked element. Nine-node and seventeen-node super-elements with linearly varying displacement between two neighboring nodes were suggested (Tong *et al.* 1973). Similar derivation based on the complex potential not using conformal mapping was suggested (Cheung and Chen 1991). A formulation of HCE was suggested, which was based on the Williams expansion form at the vicinity of a crack tip (Karihaloo and Xiao 2001, Xiao and Karihaloo 2004, 2007).

The merit of the hybrid method including HCE is to assume displacements and stresses over different parts of the continuum separately (Tong *et al.* 1973, Tong and Rossettos 1977, Atluri *et al.* 1983). One possibility in the formulation of HCE is to assume an elasticity solution in the cracked region and to assume some displacement mode along the boundary. In the assumed displacement mode along the boundary, there are some undetermined coefficients or generalized coordinates (Tong and Rossettos 1977).

Several crack problems were solved by using boundary integral equation method (Hong and Chen 1988, Chen *et al.* 1998, Chen and Hong 1999).

In the present paper, the assumed displacement mode along the boundary is called the displacement family on the element boundary. Since each term in displacement family takes a definite form of displacement along the boundary, the relevant boundary value problem can be formulated and solved by using the variational theorem. Finally, after using HCE method, the element stiffness matrix for the cracked element is obtainable. After the element stiffness matrix is obtained, the next steps are same as in the usual finite element formulation.

This paper provides a numerical solution for a finite internally cracked plate using hybrid finite element method. In the formulation, an inclined crack is placed in any place of a rectangular element. The crack face is of traction free. Based on a previous study (Chen 1983), complex potentials for the cracked rectangle are derived, which satisfy (a) all governing equations of plane elasticity, (b) the traction free condition along crack face. The complex potentials are expressed in a series form, and several undetermined coefficients are involved. As knowledge of author, those complex potentials are first suggested in this paper. Based on a variational principle, the element stiffness matrix can be evaluated. The next steps are same as in the usual finite element method. Several numerical examples with computed stress intensity factor and T-stress are presented.

2. Analysis

2.1 General for formulation of element stiffness matrix for HCE

Some formulations for HCE (hybrid crack element) were proposed by (Tong *et al.* 1973, Tong

and Rossettos 1977, Cheung and Chen 1991, Karihaloo and Xiao 2001, Xiao and Karihaloo 2004, 2007). Generally, the formulation of HCE relies on the usage a variety of variational principles in elasticity (Hu 1955, Washizu 1982). In fact, the same result for the formulation of HCE can be obtained by different ways and the final result may be the same. In order to make a complete statement for the method, a compact description for the formulation of HCE is presented below, which may have a slight difference with the those previously suggested.

It is known that the key point in the FE (finite element) formulation is to derive the element stiffness matrix by a variety of methods. In this case, without losing the generality, we can assume that the HCE is surrounded by many interelement boundaries with displacement boundary condition.

From the previously published papers (Tong *et al.* 1973, Tong and Rossettos 1977, Chen 1983, Dhanasekar *et al.* 2006, Xiao and Karihaloo 2007, Cen *et al.* 2011), the following simplified variational functional Π^e for the cracked element in Fig. 1(a) is introduced

$$\Pi^e = -\frac{1}{2} \int_{s_{in}^e} u_i \sigma_{ij} n_j ds + \int_{s_{in}^e} \tilde{u}_i \sigma_{ij} n_j ds \tag{1}$$

Here, one term cited in some references is deleted because no traction boundary for the cracked element is assumed.

In Eq. (1), s_{in}^e denotes the interelement boundaries of the cracked region Ω^e . The displacement and traction components defined in the cracked region Ω^e as well as on the boundary s_{in}^e are denoted by

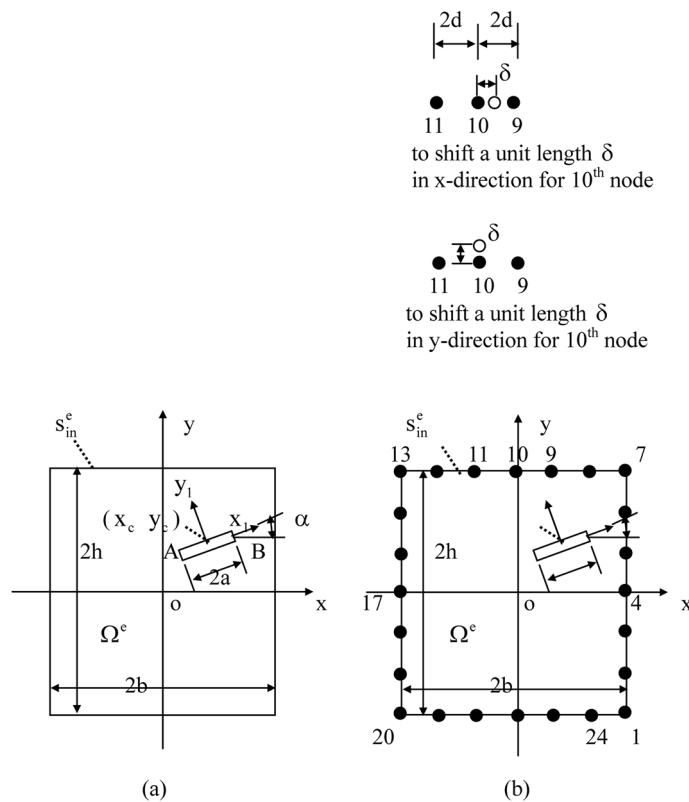


Fig. 1 (a) A rectangular cracked element, (b) boundary node arrangement for the element

u_i and σ_{ij} (Fig. 1(a)). In addition, particular displacement components \tilde{u}_i are defined on the boundary s_{in}^e only. In Eq. (1), n_j denotes the direction cosines of the outward normal with respect to a boundary point.

In the formulation, one may define and introduce two types of physical quantities. The first one is for components u_i and σ_{ij} , which is defined on the region Ω^e as well as its boundary s_{in}^e (Fig. 1(a)). We assume that those components u_i and σ_{ij} satisfy all governing equations of plane elasticity. Thus, we have used the Trefftz method in the formulation of HCE.

In the rectangular cracked element and its boundary as shown in Fig. 1(a), the displacement and stress components are expressed by the following form

$$u_i = \sum_{k=1}^{N_x} x_k u_i^{(k)}, \text{ (defined in } \Omega^e \text{ and on its boundary } s_{in}^e \text{)} \tag{2}$$

$$\sigma_{ij} = \sum_{k=1}^{N_x} x_k \sigma_{ij}^{(k)}, \text{ (defined in } \Omega^e \text{ and on its boundary } s_{in}^e \text{)} \tag{3}$$

where x_k ($k = 1, 2, \dots, n_x$) are some undetermined coefficients. In Eqs. (2) and (3), $u_i^{(k)}$ and $\sigma_{ij}^{(k)}$ are some particular elasticity solution for the cracked element (Fig. 1(a)), which will be described later in detail. In Eqs. (2) and (3), N_x is called the number of displacement-stress modes for the cracked element in the region Ω^e and on the interelement boundary s_{in}^e . In the formulation of displacement and stress family shown by Eqs. (2) and (3), the rigid motion of displacement for the element should be excluded in the summation.

The second one is for displacement component family \tilde{u}_i , which is defined along the boundary s_{in}^e only. The displacement family \tilde{u}_i can be expressed in the form

$$\tilde{u}_i = \sum_{n=1}^{N_q} q_n \tilde{u}_i^{(n)} \text{ (defined on } s_{in}^e \text{)} \tag{4}$$

where q_n ($n=1, 2, \dots, N_q$) are some undetermined coefficients, and $\tilde{u}_i^{(n)}$ ($n = 1, 2, \dots, N_q$) are some particular boundary displacement along the boundary s_{in}^e , which will be described later in detail. In Eq. (4), N_q is called the nodal displacement parameter along the boundary s_{in}^e . In the formulation, the following stability condition $N_x \geq N_q - 3$ must be satisfied (Tong *et al.* 1973, Tong and Rossettos 1977, Xiao and Karihaloo 2007).

Substituting Eqs. (2), (3) and (4) into Eq. (1) yields

$$\Pi^e = -\frac{1}{2} \sum_{k=1}^{N_x} \sum_{n=1}^{N_x} H_{kn} x_k x_n + \sum_{k=1}^{N_x} \sum_{n=1}^{N_q} G_{kn} x_k q_n \tag{5}$$

where

$$H_{kn} = H_{nk} = \int_{s_{in}^e} u_i^{(n)} \sigma_{ij}^{(k)} n_j ds, \text{ (} k, n=1, 2, \dots, N_x \text{)} \tag{6}$$

$$G_{kn} = \int_{s_{in}^e} \tilde{u}_i^{(n)} \sigma_{ij}^{(k)} n_j ds, \text{ (} k=1, 2, \dots, N_x, n=1, 2, \dots, N_q \text{)} \tag{7}$$

In Eq. (6), the relation $H_{kn} = H_{nk}$ is actually obtained from the Betti's reciprocal theorem for two elasticity solutions.

Eq. (5) may be written in a matrix representation form

$$\Pi^e = -\frac{1}{2} \mathbf{x}^T \mathbf{H} \mathbf{x} + \mathbf{x}^T \mathbf{G} \mathbf{q} \tag{8}$$

From the condition $\delta\Pi^e = 0$, or $\partial\Pi^e/\partial x_k = 0$ ($k = 1, 2, \dots, N_x$), we will find

$$\mathbf{H}\mathbf{x} = \mathbf{G}\mathbf{q} \tag{9}$$

and

$$\mathbf{x} = \mathbf{H}^{-1}\mathbf{G}\mathbf{q} \tag{10}$$

where \mathbf{H}^{-1} denotes an inverse matrix with respect to the matrix \mathbf{H} . Since the matrix \mathbf{H} is symmetry, or $H_{ij} = H_{ji}$, we have

$$\mathbf{x}^T = \mathbf{q}^T \mathbf{G}^T [\mathbf{H}^{-1}]^T = \mathbf{q}^T \mathbf{G}^T \mathbf{H}^{-1} \tag{11}$$

Substituting Eqs. (10) and (11) into Eq. (8) yields

$$\Pi^e = \frac{1}{2} \mathbf{x}^T \mathbf{G}\mathbf{q} = \frac{1}{2} \mathbf{q}^T \mathbf{K}\mathbf{q} \tag{12}$$

where

$$\mathbf{K} = \mathbf{G}^T \mathbf{H}^{-1} \mathbf{G} \tag{13}$$

This matrix \mathbf{K} is the element stiffness matrix for the HCE.

2.2 Derivation for the displacement-stress family u_i and σ_{ij} using complex variable

Derivations for the displacement-stress family shown in Eqs. (2) and (3) are introduced below, which depend on the usage of the complex variable function.

The complex variable function method plays an important role in plane elasticity. Fundamental of this method is introduced. In the method, the stresses ($\sigma_x, \sigma_y, \sigma_{xy}$), the resultant forces (X, Y) and the displacements (u, v) are expressed in terms of complex potentials $\phi(Z)$ and $\psi(Z)$ such that (Muskhelishvili 1963)

$$\begin{aligned} \sigma_x + \sigma_y &= 4\text{Re}\Phi(z), \\ \sigma_y - \sigma_x + 2i\sigma_{xy} &= 2[\bar{z}\Phi'(z) + \Psi(z)] \quad \text{or} \quad \sigma_y - \sigma_x - 2i\sigma_{xy} = 2[z\overline{\Phi'(z)} + \overline{\Psi(z)}] \end{aligned} \tag{14}$$

$$f = -Y + iX = \phi(z) + z\overline{\phi'(z)} + \overline{\psi(z)} \tag{15}$$

$$2G(u + iv) = \kappa\phi(z) - z\overline{\phi'(z)} - \overline{\psi(z)} \tag{16}$$

where $\Phi(z) = \phi'(z)$, $\Psi(z) = \psi'(z)$, a bar over a function denotes the conjugated value for the function, G is the shear modulus of elasticity, $\kappa = (3 - \nu)/(1 + \nu)$ in the plane stress problem, $\kappa = 3 - 4\nu$ in the plane strain problem, and ν is the Poisson's ratio. Sometimes, the displacements u and v are denoted by u_1 and u_2 , the stresses σ_x, σ_y and σ_{xy} by σ_1, σ_2 and σ_{12} , the coordinates x and y by x_1 and x_2 .

It is assumed that the crack center is placed at some place of a rectangular plate, and the crack has an inclined angle α . In this case, we first study the problem in the $o_1x_1y_1$ coordinates (Fig. 1(a)). The relevant complex potentials are denoted as $\phi_1(z_1)$ and $\psi_1(z_1)$ (where $z_1 = x_1 + iy_1$). From Eq. (15), the traction free condition along the crack face can be written as (Muskhelishvili 1963)

$$\phi_1(z) + z_1\overline{\phi_1'(z_1)} + \overline{\psi_1(z_1)} = 0 \quad (\text{along the crack face}) \tag{17}$$

From a previous publication, two types of the expansion forms which satisfy the condition (17) were suggested (Chen 1983). In that paper, the expansion form for $\phi_1(z)$ and $\omega_1(z)$ was obtained. In fact, from obtained complex potentials $\phi_1(z)$ and $\omega_1(z)$, the complex potential $\psi_1(z)$ can be obtained accordingly.

For two types of the expansion form, the first type can be expressed as

$$\phi_1(z_1) = \sum_{k=1}^M (a_k + ib_k)X(z_1)z_1^{k-1} \tag{18}$$

$$\psi_1(z_1) = \sum_{k=1}^M (a_k - ib_k)X(z_1)z_1^{k-1} - z_1\phi_1'(z_1) \tag{19}$$

where

$$X(z_1) = \sqrt{z_1^2 - a^2} \text{ (taking the branch } \lim_{z_1 \rightarrow \infty} X(z_1)/z_1 = 1 \text{)} \tag{20}$$

In Eqs. (18) and (19), a_k, b_k ($k=1, 2, \dots, M$) are $2M$ undetermined coefficients.

The second type is expressed as

$$\phi_1(z_1) = \sum_{k=1}^M (c_k + id_k)z_1^k \tag{21}$$

$$\psi_1(z_i) = -\sum_{k=1}^M (c_k - id_k)z_1^k - z_1\phi_1'(z_1) \tag{22}$$

In Eqs. (21) and (22), c_k, d_k ($k=1, 2, \dots, M$) are $2M$ undetermined coefficients. Note that, the pair $\phi_1(z_1) = id_1z_1, \psi_1(z_1) = id_1z_1 - z_1\phi_1'(z_1) = 0$ represents a rigid motion of body. Therefore, this pair should be excluded in the group.

From the complex potentials in the $o_1x_1y_1$ coordinates, we will obtain relevant complex potentials in the oxy coordinates by (Muskhelishvili 1963)

$$\phi(z) = e^{i\alpha}\phi_1(z_1), \psi(z) = e^{-i\alpha}\psi_1(z_1) - \bar{z}_c\phi_1'(z_1) \tag{23}$$

where

$$z_1 = e^{-i\alpha}(z - z_c) \text{ (with } z_1 = x_1 + iy_1, z = x + iy, z_c = x_c + iy_c \text{)} \tag{24}$$

We may write two types of the expansion form in the following unified form

$$\phi(z) = \sum_{m=1}^{n_x} x_m\phi^{(m)}(z), \psi(z) = \sum_{m=1}^{n_x} x_m\psi^{(m)}(z) \text{ (with } n_x = 4M - 1 \text{)} \tag{25}$$

In fact, the coefficients in Eq. (25) are composed of following coefficients

$$\{x_1x_2, \dots, x_{2M-1}x_{2M}\} = \{a_1b_1, \dots, a_Mb_M\} \tag{26}$$

$$\{x_{2M+1}x_{2M+2}, \dots, x_{4M-2}x_{4M-1}\} = \{c_1c_2d_2, \dots, a_Mb_M\} \tag{27}$$

Note that, in Eq. (27) the coefficient d_1 has been excluded. In addition, the complex potential pairs $\phi^{(m)}(z), \psi^{(m)}(z)$ ($m=1, 2, \dots, n_x = 4M - 1$) have been defined previously from Eqs. (18) to (23). From the complex potential pair $\phi^{(m)}(z), \psi^{(m)}(z)$, the relevant displacement and stress fields are denoted by $u_i^{(m)}$ and $\sigma_{ij}^{(m)}$. The proposed expansion form is used to formulate the element stiffness matrix. In the present study, we choose $M=15$ and $N_q = 59$ ($N_q = 4M - 1$). Obviously, it

is the key point to derive the displacement-stress family. Those derivations are first suggested in this paper.

2.3 Assumption for displacement family \tilde{u}_i along the boundary s_{in}^e

As claimed previously, the displacement family is expressed as $\tilde{u}_i = \sum_{n=1}^{N_q} q_n \tilde{u}^{(n)}$ (defined along s_{in}^e).

In the present study, 24 nodes are assumed along the outer boundary s_{in}^e (Fig. 1(b)). This family is obtained in the following way. Except for one node, let all nodes preserve in a fixed position. In the meantime, one allows one node, for example, the 10th node, to shift a unit length in x - or y -direction, respectively. Thus, the total undetermined coefficients in Eq. (4) is 48 (=2×24). Therefore, we have $N_q = 48$. Clearly, the stability condition $N_x \geq N_q - 3$ ($N_x = 59, N_q = 48$) is satisfied in the present study.

When the 10th node has a unit shift δ ($\delta = 1$) in x - or y -direction respectively, the relevant scheme is indicated in Fig. 1(b). This situation can be described by the following equations

$$\tilde{u}^{(19)}(s) = \delta \frac{d+s}{2d}, \text{ (for } u_1, |s| \leq d, \text{ along the interval from node "11" to "10")} \quad (28a)$$

$$\tilde{u}^{(19)}(s) = \delta \frac{d-s}{2d}, \text{ (for } u_1, |s| \leq d, \text{ along the interval from node "10" to "9")} \quad (28b)$$

$$\tilde{u}_1^{(19)}(s) = 0, \text{ (for } u_1, \text{ along other intervals on boundary)} \quad (28c)$$

and

$$\tilde{u}^{(20)}(s) = \delta \frac{d+s}{2d}, \text{ (for } u_2, |s| \leq d, \text{ along the interval from node "11" to "10")} \quad (29a)$$

$$\tilde{u}^{(20)}(s) = \delta \frac{d-s}{2d}, \text{ (for } u_2, |s| \leq d, \text{ along the interval from node "10" to "9")} \quad (29b)$$

$$\tilde{u}^{(20)}(s) = 0, \text{ (for } u_2, \text{ along other intervals on boundary)} \quad (29c)$$

Note that the expression $\tilde{u}^{(19)}(s)$ is for a unit displacement at 10th node in x -direction, and $\tilde{u}^{(20)}(s)$ is for a unit displacement at 10th node in y -direction. In a real computation, we can choose $\delta = 1$.

2.4 Solution technique

Once the element stiffness matrices for many cracked elements are obtained, the assembling of matrices can be carried out in a usual way. In addition, the applied loading can be reduced to some forces on nodes (Bathe 1996). Once all the element stiffness matrices were assembled, the three degrees of freedom from the rigid motion are eliminated by three support conditions at the boundary points.

Suppose the studied problem is composed of two cracked elements as shown in the Example 2 below (Fig. 2(b)). From the solution for problem, we can get the “ \mathbf{q} ” and “ \mathbf{x} ” vectors for two cracked element. In fact, the “ \mathbf{x} ” is composed of the coefficients, or a_k, b_k, c_k and d_k ($k = 1, 2, \dots, M$) in the expansion form shown by Eqs. (18) to (23). Finally, we can evaluate the SIFs and T-stresses at the left crack tip “A” and right crack tip “B” by (Chen *et al.* 2003, Chen *et al.* 2008)

$$(K_1 - iK_2)_A = 2(2\pi)^{1/2} \lim_{z_1 \rightarrow -a} \sqrt{z_1 + a} \phi'_1(z) = 2(\pi a)^{1/2} \sum_{k=1}^M (a_k + ib_k)(-a)^{k-1} \quad (30a)$$

$$(K_1 - iK_2)_B = 2(2\pi)^{1/2} \lim_{z_1 \rightarrow a} \sqrt{z_1 - a} \phi'_1(z) = 2(\pi a)^{1/2} \sum_{k=1}^M (a_k + ib_k)a^{k-1} \quad (30b)$$

$$T_A = 4 \sum_{k=1}^M kc_k(-a)^{k-1} \quad (31a)$$

$$T_B = 4 \sum_{k=1}^M kc_k a^{k-1} \quad (31b)$$

3. Numerical examples

Four numerical examples are introduced below. In the first example, the computed results for SIFs are compared with previously obtained results. The computed results for other three examples, particularly, the results for T-stresses, may not be available in other references. In computation, the plane strain condition is assumed, and $\nu = 0.3$.

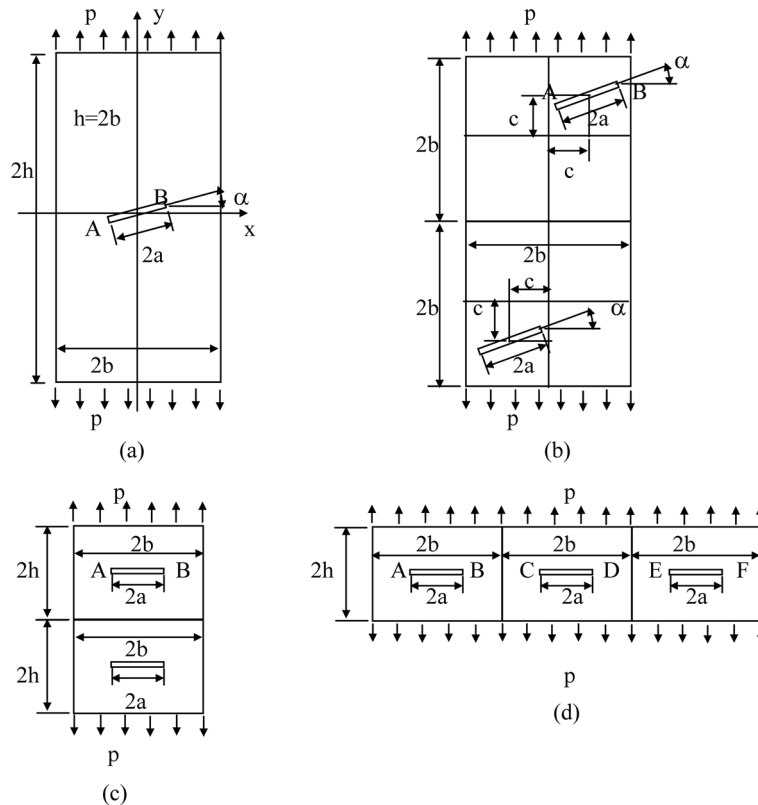


Fig. 2 (a) An incline crack in a rectangular plate, (b) two inclined crack in a rectangular plate, (c) two cracks in a stacking position in a rectangular plate, (d) three cracks in series in a rectangular plate

Example 1

In the first example, we assume that the rectangular cracked plate with ratio $h/b = 2$ has a uniform loading “p” on the two tops (Fig. 2(a)). The crack with length “2a” has an inclined angle α .

The calculated stress intensity factor and the T-stress at the tip “A” are expressed as

$$K_{1A} = F_{1A}(a/b, \alpha)p\sqrt{\pi a}, K_{2A} = F_{2A}(a/b, \alpha)p\sqrt{\pi a} \tag{32}$$

$$T_A = G_A(a/b, \alpha)p \tag{33}$$

In the case of (a) a/b changes from 0.1, 0.2, ...0.8, (c) α changes from 0, $\pi/12$, $2\pi/12$, ... to $\pi/2$, computed results for SIF and T-stress are listed in Table 1. Comparison results are also listed in Table 1.

From tabulated results, we see that in some particular cases, the SIF and T-stress can reach a comparatively larger value. For example, in the case of $a/b = 0.8$ and $\alpha = 0$, we have $F_{1A}(a/b, \alpha) = 1.7749$ and $G_A(a/b, \alpha) = -2.1281$. It is known that for a single crack in an infinite plate with remote loading $\sigma_y^\infty = p$, we have $F_{1A} = 1$ and $G_A = -1$. In addition, in the case of $\alpha = \pi/2$, we find $G_A = 1$ for all ratios of a/b . Clearly, this result coincides with the exact solution. In addition, the computed results from other source are also attached in the Table 1 (Murakami 1987). It is found that for the case of $a/b \leq 0.6$, deviations from different sources are not significant.

Example 2

In the second example, we assume that the rectangular cracked plate with two inclined cracks has

Table 1 Non-dimensional stress intensity factor $F_{1A}(a/b, \alpha)$, $F_{2A}(a/b, \alpha)$, and T-stress $G_A(a/b, \alpha)$ for a rectangular cracked plate under the loading p (see Fig. 2(a) and Eqs. (32), (33))

$F_{1A}(a/b, \alpha)$							
$\alpha =$	0	$\pi/12$	$\pi/6$	$\pi/4$	$\pi/3$	$5\pi/12$	$\pi/2$
a/b=							
0.1	1.0059	0.9388	0.7554	0.5043	0.2525	0.0677	0.0000
0.1*		0.9391	0.7557	0.5046	0.2527	0.0678	
0.2	1.0241	0.9567	0.7719	0.5172	0.2600	0.0699	0.0000
0.2*		0.9577	0.7730	0.5182	0.2605	0.0701	
0.3	1.0563	0.9879	0.7997	0.5387	0.2722	0.0735	0.0000
0.3*		0.9904	0.8025	0.5406	0.2730	0.0736	
0.4	1.1063	1.0346	0.8396	0.5689	0.2891	0.0783	0.0000
0.4*		1.0402	0.8456	0.5719	0.2896	0.0783	
0.5	1.1807	1.1003	0.8930	0.6087	0.3102	0.0840	0.0000
0.5*		1.1128	0.9046	0.6119	0.3099	0.0837	
0.6	1.2928	1.1912	0.9633	0.6597	0.3351	0.0903	0.0000
0.6*		1.2183	0.9840	0.6611	0.3332	0.0896	
0.7	1.4702	1.3193	1.0591	0.7249	0.3629	0.0966	0.0000
0.7*		1.3780	1.0910	0.7210	0.3590	0.0957	
0.8	1.7749	1.5184	1.2026	0.8063	0.3920	0.1029	0.0000
0.8*		1.6530	1.2450	0.7850	0.3880	0.1020	

*from (Murakami 1987)

Table 1 Continued

 $F_{2A}(a/b, \alpha)$

$\alpha =$	0	$\pi/12$	$\pi/6$	$\pi/4$	$\pi/3$	$5\pi/12$	$\pi/2$
$a/b =$							
0.1	0.0000	0.2502	0.4339	0.5017	0.4350	0.2514	0.0000
0.1*		0.2502	0.4339	0.5018	0.4352	0.2516	
0.2	0.0000	0.2510	0.4364	0.5066	0.4410	0.2556	0.0000
0.2*		0.2510	0.4367	0.5072	0.4417	0.2560	
0.3	0.0000	0.2529	0.4409	0.5145	0.4506	0.2623	0.0000
0.3*		0.2527	0.4417	0.5162	0.4521	0.2631	
0.4	0.0000	0.2567	0.4475	0.5252	0.4635	0.2712	0.0000
0.4*		0.2560	0.4497	0.5290	0.4660	0.2721	
0.5	0.0000	0.2644	0.4558	0.5383	0.4793	0.2816	0.0000
0.5*		0.2619	0.4617	0.5458	0.4827	0.2825	
0.6	0.0000	0.2795	0.4649	0.5540	0.4980	0.2933	0.0000
0.6*		0.2726	0.4800	0.5674	0.5022	0.2939	
0.7	0.0000	0.3081	0.4721	0.5739	0.5198	0.3056	0.0000
0.7*		0.2900	0.5080	0.5950	0.5240	0.3060	
0.8	0.0000	0.3599	0.4760	0.6022	0.5444	0.3182	0.0000
0.8*		0.3070	0.5500	0.6300	0.5490	0.3190	

*from (Murakami 1987)

 $G_A(a/b, \alpha)$

$\alpha =$	0	$\pi/12$	$\pi/6$	$\pi/4$	$\pi/3$	$5\pi/12$	$\pi/2$
$a/b =$							
0.1	-1.0067	-0.8730	-0.5070	-0.0061	0.4963	0.8649	1.0000
0.2	-1.0277	-0.8941	-0.5278	-0.0235	0.4857	0.8617	1.0000
0.3	-1.0658	-0.9307	-0.5610	-0.0503	0.4699	0.8571	1.0000
0.4	-1.1274	-0.9843	-0.6044	-0.0842	0.4514	0.8521	1.0000
0.5	-1.2245	-1.0560	-0.6551	-0.1236	0.4331	0.8483	1.0000
0.6	-1.3813	-1.1443	-0.7123	-0.1682	0.4195	0.8472	1.0000
0.7	-1.6478	-1.2466	-0.7845	-0.2174	0.4156	0.8499	1.0000
0.8	-2.1281	-1.3837	-0.9034	-0.2606	0.4269	0.8566	1.0000

a uniform loading “p” on the two tops (Fig. 2(b)). Two cracks with length “2a” have an inclined angle α .

In computation, we assume $c/b = 0.5$ and $a/b = 0.4$. The calculated stress intensity factor and the T-stress at the tips “A” and “B” are expressed as

$$\begin{aligned} K_{1A} &= F_{1A}(\alpha)p\sqrt{\pi a}, & K_{1B} &= F_{1B}(\alpha)p\sqrt{\pi a} \\ K_{2B} &= F_{2B}(\alpha)p\sqrt{\pi a}, & K_{2A} &= F_{2A}(\alpha)p\sqrt{\pi a} \end{aligned} \quad (34)$$

Table 2 Non-dimensional stress intensity factor $F_{1A}(a/b, \alpha)$, $F_{1B}(a/b, \alpha)$, $F_{2A}(a/b, \alpha)$, $F_{2B}(a/b, \alpha)$ and T-stress $G_A(a/b, \alpha)$, $G_B(a/b, \alpha)$ for a rectangular cracked plate with two inclined cracks under the loading p (see Fig. 2(b) and Eqs. (34), (35))

$\alpha =$	F_{1A}	F_{1B}	F_{2A}	F_{2B}	G_A	G_B
0	1.4718	1.6829	0.0801	-0.1094	-1.1287	-1.6751
$\pi/18$	1.4195	1.6650	0.2607	0.0939	-1.0125	-1.7630
$\pi/9$	1.2925	1.5218	0.4313	0.3737	-0.8105	-1.6312
$\pi/6$	1.0883	1.2352	0.5583	0.5872	-0.5324	-1.0153
$2\pi/9$	0.8445	0.9312	0.6162	0.6622	-0.2012	-0.4657
$5\pi/18$	0.5947	0.6429	0.6015	0.6536	0.1482	-0.0015
$\pi/3$	0.3667	0.3811	0.5180	0.5528	0.4749	0.4523
$7\pi/18$	0.1841	0.1897	0.3800	0.3992	0.7419	0.6884
$4\pi/9$	0.0570	0.0510	0.2035	0.2258	0.9221	0.8942
$\pi/2$	0.0006	0.0010	0.0000	-0.0001	0.9994	0.9916

$$T_A = G_A(\alpha)p, T_B = G_B(\alpha)p \tag{35}$$

In the case of α changing from 0, $\pi/18, 2\pi/18, \dots$ to $\pi/2$, the computed results are listed in Table 2. From tabulated results, we see that in some particular cases, the SIF and T-stress can reach a comparatively larger value. For example, in the case of $\alpha = 0$, we have $F_{1A}(\alpha) = 1.4718$, $F_{1B}(\alpha) = 1.6829$, $G_A(\alpha) = -1.1287$ and $G_B(\alpha) = -1.6751$. Simply because the tip “B” is located near the boundary, we have $F_{1B}(\alpha) > F_{1A}(\alpha)$.

Example 3

In the third second example (Fig. 2(c)), we assume that the rectangular cracked plate with two parallel cracks has a uniform loading “ p ” on the two tops. Two cracks have a length “ $2a$ ”.

In computation, we assume (a) $h/b = 0.5, 1.0, 1.5$ and 2 and (b) $a/b = 0.1, 0.2, \dots 0.9$. The computed stress intensity factor and the T-stress at the tip “A” are expressed as

$$K_{1A} = F_{1A}(h/b, a/b)p\sqrt{\pi a}, K_{2A} = F_{2A}(h/b, a/b)p\sqrt{\pi a} \tag{36}$$

$$T_A = G_A(h/b, a/b)p \tag{37}$$

The computed results are listed in Table 3. From tabulated results, we see that in some particular cases, the SIF and T-stress can reach a comparatively larger value. For example, in the case of $h/b = 0.5$ and $a/b = 0.9$, we have $F_{1A}(h/b, a/b) = 3.1934$, $F_{2A}(h/b, a/b) = 0.9827$, $G_A(h/b, a/b) = -3.4789$. On the contrary, for a shorter crack case, for example, in the case of $h/b = 0.5$ and $a/b = 0.1$, we have $F_{1A}(h/b, a/b) = 1.0245 (\approx 1)$, $F_{2A}(h/b, a/b) = 0.0036 (\approx 0)$, $G_A(h/b, a/b) = -1.0202 (\approx -1)$.

Example 4

In the fourth example (Fig. 2(d)), we assume that the rectangular cracked plate with three cracks in series has a uniform loading “ p ” on the two tops. Three cracks have a length “ $2a$ ”.

In computation, we assume (a) $h/b = 1.0, 1.5, 2.0$ and 2.5 and (b) $a/b = 0.1, 0.2, \dots 0.9$. The calculated stress intensity factor and the T-stress at the tip “A”, “B” and “C” are expressed as

$$K_{1A} = F_{1A}(h/b, a/b)p\sqrt{\pi a}, K_{1B} = F_{1B}(h/b, a/b)p\sqrt{\pi a}, K_{1C} = F_{1C}(h/b, a/b)p\sqrt{\pi a} \tag{38}$$

Table 3 Non-dimensional stress intensity factor $F_{1A}(h/b, a/b)$, $F_{2A}(h/b, a/b)$ and T-stress $G_A(h/b, a/b)$ for a rectangular cracked plate with two parallel cracks in a staking position under the loading p (see Fig. 2(c) and Eqs. (36), (37))

$a/b =$	0.1	0.2	0.3	0.4	0.5	0.6	0.7	0.8	0.9
$h/b =$									
0.5	1.0245	1.0949	1.2041	1.3473	1.5278	1.7604	2.0696	2.4946	3.1934
1.0	1.0094	1.0375	1.0851	1.1537	1.2478	1.3770	1.5643	1.8749	2.5781
1.5	1.0065	1.0265	1.0615	1.1146	1.1920	1.3059	1.4838	1.7965	2.4743
2.0	1.0059	1.0240	1.0562	1.1061	1.1805	1.2927	1.4702	1.7749	2.3681

$a/b =$	0.1	0.2	0.3	0.4	0.5	0.6	0.7	0.8	0.9
$h/b =$									
0.5	0.0036	0.0257	0.0738	0.1458	0.2385	0.3556	0.5115	0.7261	0.9827
1.0	0.0005	0.0038	0.0122	0.0265	0.0464	0.0699	0.0939	0.1132	0.1191
1.5	0.0001	0.0005	0.0015	0.0032	0.0055	0.0080	0.0102	0.0116	0.0113
2.0	0.0000	0.0000	0.0001	0.0003	0.0005	0.0007	0.0010	0.0010	0.0006

$a/b =$	0.1	0.2	0.3	0.4	0.5	0.6	0.7	0.8	0.9
$h/b =$									
0.5	-1.0202	-1.0695	-1.1240	-1.1697	-1.2224	-1.3308	-1.5745	-2.1035	-3.4789
1.0	-1.0110	-1.0439	-1.0993	-1.1805	-1.2973	-1.4736	-1.7651	-2.3237	-3.7567
1.5	-1.0079	-1.0325	-1.0761	-1.1445	-1.2493	-1.4149	-1.6966	-2.2355	-3.4457
2.0	-1.0066	-1.0274	-1.0654	-1.1269	-1.2242	-1.3815	-1.6486	-2.1292	-3.0265

$$T_A = G_A(h/b, a/b)p, T_B = G_B(h/b, a/b)p, T_C = G_C(h/b, a/b)p \quad (39)$$

The computed results are listed in Table 4. From tabulated results, we see that in some particular cases, the SIF and T-stress can reach a comparatively larger value. For example, in the case of h/b

Table 4 Non-dimensional stress intensity factor $F_{1A}(h/b, a/b)$, $F_{1B}(h/b, a/b)$, $F_{1C}(h/b, a/b)$ and T-stress $G_A(h/b, a/b)$, $G_B(h/b, a/b)$, $G_C(h/b, a/b)$ for a rectangular cracked plate with three cracks in series under the loading p (see Fig. 2(d) and Eqs. (38), (39))

$a/b =$	0.1	0.2	0.3	0.4	0.5	0.6	0.7	0.8	0.9
$h/b =$									
1.0	1.0115	1.0456	1.1003	1.1726	1.2604	1.3654	1.5018	1.7210	2.2432
1.5	1.0057	1.0230	1.0524	1.0957	1.1568	1.2450	1.3819	1.6244	2.1600
2.0	1.0049	1.0199	1.0463	1.0868	1.1467	1.2366	1.3787	1.6236	2.1044
2.5	1.0048	1.0197	1.0462	1.0872	1.1485	1.2403	1.3824	1.6145	2.0261

Table 4 Continued

$F_{1B}(h/b, a/b)$

$a/b =$	0.1	0.2	0.3	0.4	0.5	0.6	0.7	0.8	0.9
$h/b =$									
1.0	1.0114	1.0447	1.0976	1.1681	1.2564	1.3686	1.5253	1.7916	2.4464
1.5	1.0058	1.0236	1.0545	1.1008	1.1674	1.2649	1.4189	1.6993	2.3392
2.0	1.0049	1.0202	1.0474	1.0895	1.1527	1.2489	1.4044	1.6808	2.2440
2.5	1.0049	1.0198	1.0466	1.0885	1.1519	1.2485	1.4021	1.6614	2.1384

$F_{1C}(h/b, a/b)$

$a/b =$	0.1	0.2	0.3	0.4	0.5	0.6	0.7	0.8	0.9
$h/b =$									
1.0	1.0090	1.0348	1.0746	1.1254	1.1864	1.2647	1.3858	1.6273	2.2977
1.5	1.0051	1.0206	1.0477	1.0889	1.1494	1.2406	1.3891	1.6671	2.3146
2.0	1.0048	1.0197	1.0462	1.0871	1.1486	1.2427	1.3959	1.6713	2.2395
2.5	1.0047	1.0193	1.0453	1.0859	1.1476	1.2423	1.3939	1.6528	2.1353

$G_A(h/b, a/b)$

$a/b =$	0.1	0.2	0.3	0.4	0.5	0.6	0.7	0.8	0.9
$h/b =$									
1.0	-1.0138	-1.0549	-1.1192	-1.2000	-1.2945	-1.4136	-1.6012	-1.9877	-3.0755
1.5	-1.0057	-1.0243	-1.0581	-1.1114	-1.1929	-1.3220	-1.5432	-1.9699	-2.9345
2.0	-1.0042	-1.0184	-1.0464	-1.0940	-1.1717	-1.2996	-1.5180	-1.9102	-2.6391
2.5	-1.0039	-1.0170	-1.0436	-1.0895	-1.1652	-1.2885	-1.4904	-1.8210	-2.3411

$G_B(h/b, a/b)$

$a/b =$	0.1	0.2	0.3	0.4	0.5	0.6	0.7	0.8	0.9
$h/b =$									
1.0	-1.0121	-1.0413	-1.0732	-1.0906	-1.0801	-1.0370	-0.9753	-0.9728	-1.5224
1.5	-1.0049	-1.0179	-1.0357	-1.0550	-1.0740	-1.0954	-1.1412	-1.3023	-1.9373
2.0	-1.0035	-1.0126	-1.0260	-1.0429	-1.0652	-1.1012	-1.1785	-1.3736	-1.8828
2.5	-1.0032	-1.0114	-1.0242	-1.0417	-1.0680	-1.1132	-1.2014	-1.3838	-1.7542

$G_C(h/b, a/b)$

$a/b =$	0.1	0.2	0.3	0.4	0.5	0.6	0.7	0.8	0.9
$h/b =$									
1.0	-1.0068	-1.0225	-1.0348	-1.0285	-0.9917	-0.9233	-0.8439	-0.8453	-1.4741
1.5	-1.0014	-1.0052	-1.0105	-1.0162	-1.0227	-1.0353	-1.0778	-1.2445	-1.9091
2.0	-1.0012	-1.0048	-1.0109	-1.0201	-1.0352	-1.0656	-1.1399	-1.3375	-1.8663
2.5	-1.0012	-1.0046	-1.0109	-1.0215	-1.0414	-1.0814	-1.1673	-1.3541	-1.7466

= 1.0 and $a/b = 0.9$, we have $F_{1A}(h/b, a/b) = 2.2432$ (at tip “A”), $F_{1B}(h/b, a/b) = 2.4464$ (at tip “B”) and $F_{1C}(h/b, a/b) = 2.2977$ (at tip “C”). Clearly, three values for SIF are in the same level. However, in the same condition of $h/b = 1.0$ and $a/b = 0.9$, for the T-stress, we have $G_A(h/b, a/b) = -3.0755$ (at tip “A”), $G_B(h/b, a/b) = -1.5224$ (at tip “B”) and $G_C(h/b, a/b) = -1.4741$. Clearly, three values for T-stress are not in the same level.

4. Conclusions

Some particular features in the present study are emphasized. First of all, the crack in an element can be located in an arbitrary position with an arbitrary inclined angle. By using complex variable method, the displacement-stress family u_i and σ_{ij} in the cracked rectangle are derived accordingly. In the author’s knowledge, this formulation can only be achieved by using the complex variable method in the crack problem (Chen 1983). In an earlier formulation by Chen (1983), the crack is located in a horizontal position. Therefore, the way for deriving the complex potentials in this paper is more difficult than in the previous case.

This paper provides the expansion form of complex potentials shown by Eqs. (18) to (23), which are key points in the present study. As claimed above, the obtained expansion form satisfies: (a) traction free condition along crack, (b) all governing equations of plane elasticity. Thus, the assumed displacement-stress state within the cracked element belongs a type of Trefftz formulation. Particularly, for such a complicated case, or an inclined crack in any position of rectangular element, the mentioned displacement-stress family is impossible to obtain by real variable analysis. The computed results in this paper provide not only the SIF but also the higher order term, for example, the T-stress component.

Usually, in the boundary value problem of a single crack in cracked plate, the boundary collocation technique was used. It is known that the collocation scheme may affect the computed results. However, the variational principle is used in the HCE method. Therefore, using HCE method is more reasonable for the studied problem.

Secondly, sufficient terms for the displacement-stress family are adopted in formulation. This will model the stress field for the cracked rectangle more accurately. For the single crack case shown by Fig. 2(a), the comparison has been made for different sources of computation. It is proved from tabulated results in Table 1 that the computed results in this paper are sufficient accurate.

References

- Atluri, S.N., Gallagher, R.H. and Zienkiewicz, O.C. (Ed.) (1983), *Hybrid and Mixed Finite Element Methods*, John Wiley & Son, Chichester.
- Bathe, K.J. (1996), *Finite Element Procedures*, Prentice-Hall, Englewood-Cliffs.
- Cen, S., Zhou, M.J. and Fu, X.R. (2011), “A 4-node hybrid stress-function (HS-F) plane element with drilling degrees of freedom less sensitive to severe mesh distortions”, *Comput. Struct.* **89**, 517-528.
- Chen, J.T., Chen, K.H. Yeih, W. and Shieh, N.C. (1998), “Dual boundary element analysis for cracked bars under torsion”, *Eng. Comput.*, **15**, 732-749.
- Chen, J.T. and Hong, H.K. (1999), “Review of dual boundary element methods with emphasis on hypersingular integrals and divergent series”, *ASME Appl. Mech. Rev.*, **52**, 17-33.
- Chen, Y.Z. (1983), “An investigation of the stress intensity factor for a finite internally cracked plate by using

- variational method”, *Eng. Fract. Mech.* **17**, 387-394.
- Chen, Y.Z., Hasebe, N. and Lee, K.Y. (2003), *Multiple Crack Problems in Elasticity*, WIT Press, Southampton.
- Chen, Y.Z., Lin, X.Y. and Wang, Z.X. (2008), “Evaluation of the T-stress and stress intensity factor for a cracked plate in general case using eigenfunction expansion variational method”, *Fatigue Fract. Eng. Mat. Struct.*, **31**, 478-487.
- Cheung, Y.K. and Chen, Y.Z. (1991), “Hybrid finite element formulation in plane elasticity by using complex variable function”, *Proceedings of the Asian Pacific Conference on Computational Mechanics*, 1149-1155.
- Choi, N., Choo, Y.S. and Lee, B.C. (2006), “A hybrid Trefftz plane elasticity element with drilling degrees of freedom”, *Comput. Meth. Appl. Mech. Eng.*, **195**, 4095-4105.
- Day, M.L. and Yang, T.Y. (1982), “A mixed variational principle for finite element analysis”, *Int. J. Numer. Meth. Eng.*, **18**, 1213-1230.
- Dhanasekar, M., Han, J.J. and Qin, Q.H. (2006), “A hybrid-Trefftz element containing an elliptic hole”, *Finite Elem. Anal. Des.*, **42**, 1314-1323.
- Hong, H.K. and Chen, J.T. (1988), “Derivations of integral equations of elasticity”, *ASCE J. Eng. Mech.* **6**, 1028-1044.
- Hu, H.C. (1955), “On some variational principles in the theory of elasticity and plasticity”, *Scientia Sinica*, **4**, 33-54.
- Karihaloo, B.L. and Xiao, Q.Z. (2001), “Accurate determination of the coefficients of elastic tip asymptotic field by a hybrid crack element with p-adaptivity”, *Eng. Fract. Mech.*, **68**, 1609-1630.
- Long, Y.Q., Cen, S. and Long, Z.F. (2009), *Advanced Finite Element Method in Structural Engineering*, Springer-Verlag GmbH, Tsinghua University Press Berlin, Heidelberg, Beijing.
- Muskhelishvili, N.I. (1963), *Some Basic Problems of Mathematical Theory of Elasticity*, Noordhoff, Groningen.
- Murakami, Y. (1987), *Stress Intensity Factors Handbook*, Vol. 2, Pergamon, Oxford.
- Pian, T.H.H. (1964), “Derivation of element stiffness matrices by assumed stress distribution”, *AIAA J.*, **2**, 1333-1336.
- Pian, T.H.H. and Chen, D.P. (1982), “Alternative ways for formulation of hybrid stress elements”, *Int. J. Numer. Meth. Eng.*, **18**, 1679-1684.
- Pian, T.H.H., Chen, D.P. and King, D. (1983), “A new formulation of hybrid/mixed finite element”, *Comput. Struct.*, **16**, 1-4.
- Sze, K.Y., Liu, G.H. and Fan, H. (2010), “Four- and eight-node hybrid-Trefftz quadrilateral finite element models for helmholtz problem”, *Comput. Meth. Appl. Mech. Eng.*, **199**, 598-614.
- Tong, P., Pian, T.H.H. and Lasry, S.J. (1973), “A hybrid-element approach to crack problems in plane elasticity”, *Int. J. Numer. Meth. Eng.*, **7**, 297-308.
- Tong, P. and Rossettos, J.N. (1977), *Finite-element Method*, The MIT Press, Cambridge.
- Washizu, K. (1982), *Variational Methods in Elasticity and Plasticity* Pergamon, Oxford.
- Wisniewski, K. and Turska, E. (2009), “Improved 4-node Hu–Washizu elements based on skew coordinates”, *Comput. Struct.*, **87**, 407-424.
- Xiao, Q.Z., Karihaloo, B.L. and Liu, X.Y. (2004), “Direct determination of SIF and higher order terms of mixed mode cracks by a hybrid crack element”, *Inter. J. Fract.*, **125**, 207-225.
- Xiao, Q.Z., Karihaloo, B.L. (2007), “Implementation of hybrid crack element on a general finite element mesh and in combination with XFEM”, *Comput. Meth. Appl. Mech. Eng.*, **196**, 1864-1873.